A General Framework for the Calculation of Average Outage Duration of Diversity Systems over Generalized Fading Channels

Young-Chai Ko, *Member, IEEE*,

Ali Abdi, *Member, IEEE*,

Mohamed-Slim Alouini, *Member, IEEE*, and

Mostafa Kaveh, *Fellow, IEEE*.

This is an expanded version of work which was presented at the IEEE Wireless Commun. and Net. Conf. (WCNC'2000), Chicago, IL, September 2000. This work was supported by the National Science Foundation under grants CCR-9983462 and ECS-9979443. Y. -C. Ko is with the Texas Instruments, Inc., San Diego Wireless center, 5505 Morehouse Drive, CA 92121. A. Abdi is with the Dept. of Electrical and Computer Engineering, New Jersey Institute of Technology, 323 King Blvd. Newark, NJ 07102. M.-S. Alouini and M. Kaveh are with the Department of Electrical and Computer Engineering, University of Minnesota, Minneapolis, MN 55455, USA. Y. -C. Ko can be reached at Tel: (858) 404-6427, Fax: (858) 678-0501, and E-mail: <yko@ti.com>. A. Abdi can be reached at Tel: (973) 596-5621, Fax: (973) 596-5680, and E-mail: <ali.abdi@njit.edu>. M.-S. Alouini can be reached at Tel: (612) 625-9055, Fax: (612) 625-4583, and E-mail: <alouini@ece.umn.edu>. M. Kaveh can be reached at Tel: (612) 625-0720, Fax: (612) 625-4583, and E-mail: <kaveh@ece.umn.edu>.

Abstract

This paper presents two approaches for the calculation of the average outage duration (AOD) of diversity systems over generalized fading channels. First, a "classical" probablility density function (PDF)-based approach, is used to obtain exact closed form expressions for the AOD of maximal-ratio combiner (MRC) over independent and identically distributed (i.i.d.) Rayleigh and Rice fading channels. On the other hand, relying upon a numerical technique for inverting Laplace transforms of CDFs, and in conjunction with the calculation of the joint characteristic function (CF) of the combined output SNR process and its time derivative, a CF-based approach is adopted to compute the AOD of MRC over non-i.i.d. Rayleigh and Rician diversity paths. The mathematical expressions are ilustrated by presenting and interpreting numerical results/plots, showing the impact of the power delay profile, the angle of arrivals, and the angle spreads on the AOD of diversity systems operating over typical fading channels of practical interest.

I. Introduction

The problem of fading and its deleterious impact on the performance of wireless communication systems has been of interest for a long time. To mitigate fading many communication systems make use of diversity schemes in one form or another [1], [2], [3]. Average probability of error has been traditionally the most commonly used performance measure of these diversity schemes [4], [5]. However, in certain communication system applications such as adaptive transmission schemes [6], [7], [8], [9] the average probability of error does not provide enough information for the overall system design and configuration. In that case, in addition to the average probability of error, wireless communication design engineers are also interested in other performance measures such as outage probability, average outage duration (AOD), and frequency of outages.

In what follows, we provide a summary of the previous works on the AOD and level crossing rate (LCR) (related to the frequency of outages and AOD) of diversity systems. The LCR of an L branch predetection equal gain combiner (EGC) and the LCR and AOD for two-branch EGC with correlated Rayleigh signals are studied in [10] and [11], respectively. In [12], the LCR and AOD of two-branch maximal ratio combiner (MRC), EGC, and selection combiner (SC) have been analyzed and compared for Rayleigh fading. Note that the LCR and AOD expressions of [11] and [12] are accurate but approximate results and hold for branches with average equal power. More recently, [13], [14] have studied the LCR and AOD of MRC and EGC, for independent identically distribued (i.i.d.) Rayleigh fading paths. In [14], the

LCR and AOD expressions over Nakagami-m fading channels are derived for a single branch receiver, while the LCR and AOD expressions for an L branch MRC, operating over i.i.d. Nakagami-m distributed paths, are presented in [15]. The LCR of an L branch MRC with non-i.i.d. Rayleigh and Rician is caluculated in [16].

The objective of this paper is to present exact anaytical methods for calculating the AOD of diversity receivers over generalized fading channels, where diversity branches have different fading statistics. More specifically, after introducing the channel model in Section II we present two approaches for the calculation of the AOD. First, in Section III a "classical" probablility density function (PDF)-based approach, relying on the cumulative distribution function (CDF) of the combined output SNR, as well as the joint PDF of the combined output SNR and its time derivative, is used to obtain exact closed-form expressions for the LCR and AOD of MRC over i.i.d. Rayleigh and Rician fading channels. On the other hand, based on a numerical technique for inverting the Laplace transform of a CDF, along with the use of the joint characteristic function (CF) of the combined output SNR and its time derivative, a CF-based approach is adopted in Section IV. The CF-based approach allows us to calculate, numerically, the LCR and AOD of MRC over non i.i.d. Rayleigh and Rician paths. The paper illustrates the mathematical formalism by presenting and interpreting various numerical results/plots, which show the impact of the power delay profile (PDP) and the distribution of the angle of arrival (AOA) of waves on the LCR and AOD of diversity systems, operating over typical fading channels of practical interest. Finally, Section V summarizes the main contributions of the paper.

II. Generalized Fading Channels

A. *Diversity Channel Model*

In this model, L replicas $\{r_l(t)\}_{l=1}^{L}$ are received over independent paths. Because of the slow-fading assumption, the fading amplitudes $\{\alpha_l(t)\}_{l=1}^{L}$ and the AOAs $\{\theta_l(t)\}_{l=1}^{L}$ (in the horizontal plan) are all constant (time-independent) random variable over a symbol interval [2]. In our channel model, $\{\alpha_l(t)\}_{l=1}^{L}$ are independent variables, distributed according to Rayleigh and/or Rician fading distributions, described in the sequel. By definition we have $\Omega_l = E[\alpha_l^2]$, where $E[\cdot]$ denotes mathematical expectation. Moreover, $\{\theta_l(t)\}_{l=1}^{L}$ are independent variables with von Mises distribution, defined later on.

After passing through the fading channel, each replica of the signal is perturbed by the complex baseband additive white Gaussian noise (AWGN) $n_l(t)$ with the one-sided power spectral density N_l (W/Hz). The AWGN $n_l(t)$ is assumed to be statistically independent from path to path and independent of $\{r_l(t)\}_{l=1}^{L}$. Hence the instantaneous SNR per symbol of the lth path is given by $\gamma_l(t) = \frac{\alpha_l^2(t)\ E_s}{N_0}$, where E_s (J) is the energy per symbol, and $N_0 = \sum_{l=1}^{L} N_l$ (W/Hz) is the total power spectral density of $\{n_l(t)\}_{l=1}^{L}$.

B. Fading Models

For the Rayleigh fading the instantaneous SNR per symbol of the lth path, γ_l, is distributed according to an exponential distribution given by

$$p_{\gamma_l}(\gamma_l; \overline{\gamma}_l) = \frac{1}{\overline{\gamma}_l} \exp\left(-\frac{\gamma_l}{\overline{\gamma}_l}\right); \quad \gamma_l \geq 0, \tag{1}$$

where $\overline{\gamma}_l = \frac{\Omega_l E_s}{N_0}$ denotes the average SNR per symbol of the lth path. On the other hand, for the Rician fading case the distribution of γ_l, is given by

$$p_{\gamma_l}(\gamma_l; \overline{\gamma}_l, K_l) = \frac{(1+K_l)\ e^{-K_l}}{\overline{\gamma}_l} \exp\left(-\frac{(1+K_l)\ \gamma_l}{\overline{\gamma}_l}\right)\ I_0\left(2\sqrt{\frac{K_l(1+K_l)\ \gamma_l}{\overline{\gamma}_l}}\right); \quad \gamma_l \geq 0. \tag{2}$$

where K_l is the Rician factor and $I_n(\cdot)$ is the nth-order modified Bessel function of the first kind.

C. Distribution of the Angle of Arrivals

As was mentioned previously, we assume that the AOA of the lth path in the horizontal plane follows a von Mises distribution [17]

$$p_{\theta_l}(\theta_l) = \frac{\exp[\kappa_l \cos(\theta_l - \mu_l)]}{2\pi I_0(\kappa_l)}; \quad \theta_l = [-\pi, \pi) \tag{3}$$

where $\mu_l \in [-\pi, \pi)$ represents the mean direction of the AOA, and $\kappa_l \geq 0$ controls the width of AOA. For $\kappa_l = 0$, we obtain $p_{\theta_l}(\theta_l) = 1/2\pi$ (isotropic scattering), while $\kappa_l = \infty$ yields $p_{\theta_l}(\theta_l) = \delta(\theta_l - \mu_l)$ (extremely non-isotropic scattering), where $\delta(\cdot)$ is the Dirac delta function. For large κ_l the von Mises PDF converges to a Gaussian PDF with mean μ_l and standard deviation $1/\sqrt{\kappa_l}$ [18].

D. Spectral Moments

If we assume that θ_l is a von Mises variable with parameters μ_l and κ_l, then the autocovariance of $r_l(t)$, defined as $\frac{1}{2}E[r_l^*(t)r_l(t+\tau)] - |E[r_l(t)]|^2$ [2], can be shown to be [17]

$$C_{r_l r_l}(\tau) = b_{l,0} \frac{I_0\left(\sqrt{\kappa_l^2 - 4\pi^2 f_d^2 \tau^2 + j4\pi\kappa_l \cos(\mu_l) f_d \tau}\right)}{I_0(\kappa_l)}, \tag{4}$$

where $b_{l,n}$ is the nth spectral moment given by

$$b_{l,n} = \frac{1}{j^n} \frac{d^n C_{r_l r_l}(\tau)}{d\tau^n} |_{\tau=0} \; ; \quad n = 0, 1, 2, \cdots. \tag{5}$$

As we will see later, we need the first and second spectral moments for LCR calculations which can be obtained in closed form with the help of [19] by substituting (4) into (5) for $n = 1, 2$

$$\begin{cases} b_{l,1} = b_{l,0} \frac{2\pi f_d \cos(\mu_l) I_1(\kappa_l)}{I_0(\kappa_l)}, \\ b_{l,2} = b_{l,0} \frac{2\pi^2 f_d^2 [I_0(\kappa_l) + I_2(\kappa_l)\cos(2\mu_l)]}{I_0(\kappa_l)}. \end{cases} \tag{6}$$

For $\kappa_l = 0$, (4) simplifies to the correlation function of the Clarke's two-dimensional isotropic scattering model

$$C_{R_l R_l}(\tau) = b_{l,0} J_0(2\pi f_d \tau), \tag{7}$$

where $J_0(\cdot)$ is the zeroth-order Bessel function of the first kind. Furthermore, the $b_{l,1}$ and $b_{l,2}$ reduces to [2]

$$\begin{cases} b_{l,1} = 0, \\ b_{l,2} = b_{l,0} 2\pi^2 f_d^2. \end{cases} \tag{8}$$

III. PDF-Based Approach

The common approach for calculating the LCR of a real stationary random process $X(t)$, for a given threshold x_{th}, is to employ Rice's formula given by [2]

$$\begin{aligned} N_X(x_{\mathrm{th}}) &= \int_0^\infty \dot{x} \, p_{X\dot{X}}(x_{\mathrm{th}}, \dot{x}) \, d\dot{x}, \\ &= p_X(x_{\mathrm{th}}) \int_0^\infty \dot{x} \, p_{\dot{X}|X}(\dot{x}|X = x_{\mathrm{th}}) \, d\dot{x}, \end{aligned} \tag{9}$$

where $N_X(x_{\mathrm{th}})$ represents the average number of times, per unit time, that $X(t)$ crosses the threshold with positive slope, dot denotes differentiation with respect to time, $p_{X\dot{X}}(x, \dot{x})$ is the joint PDF of the random variables $X = X(t_0)$ and $\dot{X} = \dot{X}(t_0)$, where t_0 is an arbitrary instant of time, $p_X(x)$ is the PDF of the variable X, and $p_{\dot{X}|X}(\dot{x}|X = x_{\text{th}})$ is the PDF of $\dot{X}$ conditioned on $X = x_{\text{th}}$. If $\dot{X}$ is Gaussian, independent of X, with zero mean and the variance $\sigma^2_{\dot{X}}$, then (9) becomes

$$N_X(x_{\text{th}}) = \frac{\sigma_{\dot{X}}}{\sqrt{2\pi}} p_X(x_{\text{th}}). \tag{10}$$

The AOD of X_t, $T_X(x_{\text{th}})$, which indicates how long in average the random process $X(t)$ stays below the given threshold x_{th}, is given for a positive random process by [2]

$$T_X(x_{\text{th}}) = \frac{\text{Prob}[0 \le X \le x_{\text{th}}]}{N_X(x_{\text{th}})} = \frac{\int_0^{x_{\text{th}}} p_X(x)dx}{N(x_{\text{th}})}, \tag{11}$$

where $\text{Prob}[X \le x_{\text{th}}]$ is the CDF of X, also known as the outage probability of $X(t)$ for the threshold x_{th}.

A. Application to MRC over I.I.D. Rayleigh and Rician Distributed Fading Channels

Consider MRC (or equivalently, a postdetection EGC) receiver, operating over L i.i.d. fading paths. In the presence of AWGN and for equally likely transmitted symbols, the total instantaneous SNR per symbol at the output of both MRC and postdetection EGC is given by [2]

$$\gamma(t) = \sum_{l=1}^{L} \gamma_l(t) = \frac{E_s}{N_0} \sum_{l=1}^{L} \alpha_l^2(t) = \frac{E_s}{N_0} \alpha^2(t). \tag{12}$$

It is easy to verify that $\dot{\alpha}$ is a zero-mean Gaussian variable with variance $\sigma^2_{\dot{\alpha}} = (b_{1,0}b_{1,2} - b_{1,1}^2)/b_{1,0}$ [1], [20]. Hence, according to (10), the LCR of $\alpha(t)$ is given by

$$N_\alpha(\alpha_{\text{th}}) = \sqrt{\frac{b_{1,0}b_{1,2} - b_{1,1}^2}{2\pi b_{1,0}}} p_\alpha(\alpha_{\text{th}}). \tag{13}$$

A.1 Rayleigh Fading

Following the result given in [21, Appendix 5A.3] for $p_\alpha(\alpha)$, (13) can be written as

$$N_\alpha(\alpha_{\text{th}}) = \sqrt{\frac{b_{1,0}b_{1,2} - b_{1,1}^2}{2\pi b_{1,0}}} \frac{2\alpha_{\text{th}}^{2L-1}}{(L-1)!(2b_{1,0})^L} \exp\left(-\frac{\alpha_{\text{th}}^2}{2b_{1,0}}\right), \tag{14}$$

By employing the relation $\gamma_{\text{th}} = \frac{E_s}{N_0}\alpha_{\text{th}}^2$ and $\Omega_1 = E[\alpha_1^2] = 2b_{1,0}$, the LCR of γ_t can be shown to be given by

$$N_\gamma(\gamma_{\text{th}}) = \sqrt{\frac{b_{1,2}}{b_{1,0}} - \left(\frac{b_{1,1}}{b_{1,0}}\right)^2} \frac{\Omega_1}{2\sqrt{\pi}(L-1)!} \left(\frac{\gamma_{\text{th}}}{\bar{\gamma}_1}\right)^{L-1/2} \exp\left(-\frac{\gamma_{\text{th}}}{\bar{\gamma}_1}\right). \tag{15}$$

For isotropic scattering, (15) can be simplified by substituting $b_{1,1}$ and $b_{1,2}$ given in (8) as

$$N_\gamma(\gamma_{\rm th}) = \frac{\sqrt{2\pi} f_d \left(\frac{\gamma_{\rm th}}{\bar{\gamma}_1}\right)^{L-\frac{1}{2}}}{(L-1)! \exp\left(\frac{\gamma_{\rm th}}{\bar{\gamma}_1}\right)}. \tag{16}$$

(16) has been derived in [22] and [23], independently. For L=1, (16) further simplifies to the result given in [2, Eq. (2.86)]. By calculating the CDF of $p_\alpha(\alpha)$ using [19, Section 3.381] and then substituting the result, together with (15), into (11), we obtain the AOD of $\gamma(t)$ as

$$T_\gamma(\gamma_{\rm th}) = \frac{\sqrt{2\pi b_0}(L-1)! \left[\exp\left(\frac{\gamma_{\rm th}}{\bar{\gamma}_1}\right) - \sum_{l=0}^{L-1} \frac{\left(\frac{\gamma_{\rm th}}{\bar{\gamma}_1}\right)^l}{l!}\right]}{\sqrt{b_0 b_2 - b_1^2}\left(\frac{\gamma_{\rm th}}{\bar{\gamma}_1}\right)^{L-\frac{1}{2}}}. \tag{17}$$

For isotropic scattering, (17) reduces to

$$T_\gamma(\gamma_{\rm th}) = \frac{(L-1)! \left[\exp\left(\frac{\gamma_{\rm th}}{\bar{\gamma}_1}\right) - \sum_{l=0}^{L-1} \frac{\left(\frac{\gamma_{\rm th}}{\bar{\gamma}_1}\right)^l}{l!}\right]}{\sqrt{2\pi} f_d \left(\frac{\gamma_{\rm th}}{\bar{\gamma}_1}\right)^{L-\frac{1}{2}}}. \tag{18}$$

(18) has been derived in [22] and [23], independently.

In the case where $L = 1$, (18) agrees with [2, Eq. (2.95)]. For the dual branch case (L=2) with isotropic scattering, (18) simplifies to the result of [12, Eq. (18)]. Furthermore, for small values of $\gamma_{\rm th}$, using the series representation of the exponential function, it can be shown that (18) reduces to the asymptotic result given in [13, Section IV].

As a numerical example, Fig. 1 shows the effect of nonisotropic scattering with two scattering scenarios $(\mu_1, \kappa_1) = (0°, 1.2)$ and $(\mu_1, \kappa_1) = (0°, 3.3)$ over Rayleigh fading channels with diversity order L=1, 2, and 4. The above values of μ_1 and κ_1 are taken from the real measured data presented in [17]. As expected, the AOD decreases as the diversity increases. For example, when $\gamma_{\rm th}/\gamma_1 = -5$ dB, the normalized AOD with $\kappa = 1.2$ is 1.25, 1, and 0.3981 for L=1, 2, and 4, respectively. On the other hand, one can see from Fig.1 that there is a significant effect of non-isotropic scattering on the AOD. It shows that for high non-isotropic scattering, i.e., high κ, the AOD becomes large. This can be attributed to the fact that as κ increases, the correlation between the envelope samples, which is proportional to $|C_{r_l r_l}(\tau)|^2$ [2], increases. Hence, when fade (outage) occurs, it tends to last longer, which increases the AOD.

A.2 Rician Fading

Similar to the Rayleigh case, the LCR in the Rician isotropic scattering scenario is found to be given by

$$N_\gamma(\gamma_{\text{th}}) = f_d\sqrt{2\pi LK}\left(\frac{(K+1)\gamma_{\text{th}}}{LK\bar{\gamma}_1}\right)^{\frac{L}{2}}\exp\left(-\frac{K+1}{\bar{\gamma}_1}\gamma_{\text{th}}-LK\right)I_{L-1}\left(2\sqrt{\frac{LK(K+1)\gamma_{\text{th}}}{\bar{\gamma}_1}}\right). \quad (19)$$

On the other hand, the CDF of the envelope with L branch MRC over Rician fading channel can be derived with the help of [21, Appendix 5A.5] as

$$\text{Prob}[0 \leq \gamma \leq \gamma_{\text{th}}] = 1 - Q_L\left(\sqrt{2LK}, \sqrt{\frac{2(K+1)}{\bar{\gamma}_1}\gamma_{\text{th}}}\right). \quad (20)$$

where $Q_L(\cdot,\cdot)$ is the generalized (Lth-order) Marcum Q-function [21]. After substituting (20) and (19) in (11), the AOD over i.i.d. Rician fading channel can be found in closed-form as

$$\begin{aligned} T_\gamma(\gamma_{\text{th}}) &= \left(\frac{(K+1)\gamma_{\text{th}}}{LK\bar{\gamma}_1}\right)^{-\frac{L}{2}}\exp\left(-\frac{K+1}{\bar{\gamma}_1}\gamma_{\text{th}}-LK\right) \\ &\times \frac{1-Q_L\left(\sqrt{2LK}, \sqrt{\frac{2(K+1)}{\bar{\gamma}_1}\gamma_{\text{th}}}\right)}{f_d\sqrt{2\pi LK}I_{L-1}\left(2\sqrt{\frac{LK(K+1)}{\bar{\gamma}_1}\gamma_{\text{th}}}\right)}. \end{aligned} \quad (21)$$

Note that for $L = 1$, (21) reduces to the non-diversity result given in [2, Eq. (2.93)], as expected. Fig. 2 shows the normalized LCR, $N_\gamma(\gamma_{\text{th}})/f_d$ and AOD, $T_\gamma(\gamma_{\text{th}})f_d$ with MRC and postdetection EGC reception versus normalized power threshold, $\gamma_{\text{th}}/\bar{\gamma}_1$, over i.i.d. Rician fading channels with Rician factor K=3 dB, for various values of L. As expected, the AOD decreases as the order of diversity L increases. For example, for $\gamma_{\text{th}} = 0$ dB and K=3 dB, one requires 18 dB of the average SNR for a single branch and 4 dB, -1 dB, and -3 dB for L=2, 3, and 4, respectively, to achieve 0.1 normalized AOD.

B. Application to Coherent EGC over Non-I.I.D. Rayleigh Fading Channels

For coherent EGC with equally likely transmitted symbols, the combined SNR per symbol γ is given by [2, p. 249, eq. (5.108)]

$$\gamma(t) = \frac{\alpha^2 E_s}{LN_0}, \quad (22)$$

where

$$\alpha = \sum_{l=1}^{L} \alpha_l, \tag{23}$$

and α_l in (23) is Rayleigh distributed. Knowing that $\dot{\alpha}_l$ is a zero-mean Gaussian variable with variance $\sigma_{\dot{\alpha}}^2 = (b_{l,0}b_{l,2} - b_{l,1}^2)/b_{l,0}$, $\dot{\alpha} = \sum_{l=1}^{L} \dot{\alpha}_l$ can be found to be a zero-mean Gaussian variable with variance

$$\sigma_{\dot{\alpha}}^2 = \sum_{l=1}^{L} \frac{b_{l,0}b_{l,2} - b_{l,1}^2}{b_{l,0}}. \tag{24}$$

Using (10) the LCR of α can be shown to be given by

$$\begin{aligned} N_\alpha(\alpha_{\text{th}}) &= \frac{\sigma_{\dot{\alpha}}}{\sqrt{2\pi}} p_\alpha(\alpha_{\text{th}}) \\ &= \frac{\sqrt{\frac{b_{l,0}b_{l,2} - b_{l,1}^2}{b_{l,0}}}}{\sqrt{2\pi}} p_\alpha(\alpha_{\text{th}}), \end{aligned} \tag{25}$$

where $p_\alpha(\alpha)$ is the PDF of α in (23). By employing the relation, $\alpha_{\text{th}} = \sqrt{L\gamma_{\text{th}}/(E_s/N_0)}$, the LCR of γ can be shown to be

$$N_\gamma(\gamma_{\text{th}}) = \frac{\sqrt{\frac{b_{l,0}b_{l,2} - b_{l,1}^2}{b_{l,0}}}}{\sqrt{2\pi}} p_\alpha\left(\sqrt{L\gamma_{\text{th}}/(E_s/N_0)}\right). \tag{26}$$

For the dual branch case ($L = 2$), the PDF of α in (26) can be found in closed-form as [24]

$$\begin{aligned} p_\alpha(\alpha) &= \frac{2\alpha\left(\Omega_1 e^{-\frac{\alpha^2}{\Omega_1}} + \Omega_2 e^{-\frac{\alpha^2}{\Omega_2}}\right)}{(\Omega_1 + \Omega_2)^2} + \frac{2\sqrt{\pi\Omega_1\Omega_2}}{(\Omega_1 + \Omega_2)^{3/2}} e^{-\frac{\alpha^2}{\Omega_1 + \Omega_2}} \left(\frac{2\alpha^2}{\Omega_1 + \Omega_2} - 1\right) \\ &\times \left[1 - Q\left(\alpha\sqrt{\frac{2\Omega_1}{\Omega_2(\Omega_1 + \Omega_2)}}\right) - Q\left(\alpha\sqrt{\frac{2\Omega_2}{\Omega_1(\Omega_1 + \Omega_2)}}\right)\right], \end{aligned} \tag{27}$$

where $Q(\cdot)$ is the Gaussian Q-function. In addition, the CDF of γ can also be found in closed-form as [24]

$$\begin{aligned} P_\gamma(\gamma) &= 1 - \frac{\bar{\gamma}_1 e^{-\frac{2\gamma}{\bar{\gamma}_1}} + \gamma_2 e^{-\frac{2\gamma}{\bar{\gamma}_2}}}{\bar{\gamma}_1 + \bar{\gamma}_2} - \frac{2\sqrt{2\bar{\gamma}_1\bar{\gamma}_2\pi\gamma}}{(\bar{\gamma}_1 + \bar{\gamma}_2)^{3/2}} e^{-\frac{2\gamma}{\bar{\gamma}_1 + \bar{\gamma}_2}} \\ &\times \left[1 - Q\left(2\sqrt{\frac{\bar{\gamma}_1\gamma}{\bar{\gamma}_2(\bar{\gamma}_1 + \bar{\gamma}_2)}}\right) - Q\left(2\sqrt{\frac{\bar{\gamma}_2\gamma}{\bar{\gamma}_1(\bar{\gamma}_1 + \bar{\gamma}_2)}}\right)\right], \end{aligned} \tag{28}$$

and as a result the AOD of dual-branch of EGC can be obtained in closed-form. For arbitrary $L > 2$, no explicit closed expression is known for the PDF and CDF of the sum of Rayleigh or Rice RVs. Hence computation of the LCR and AOD for EGC with $L > 2$ has to rely on numerical techniques for the evaluation of such PDFs and CDFs [25], [26], [27].

IV. CF-Based Approach

A. Outline of CF-Based Approach

For diversity systems operating over generalized fading channels with non-i.i.d. paths, it is very hard, if not impossible, to derive an expression for the joint PDF of the signal envelope and its derivative at the output of the diversity combiner. Hence we express $N_X(x_{\text{th}})$ in (9) in terms of the joint CF of X and $\dot{X}$, $\Phi_{X\dot{X}}(\omega_1,\omega_2) = E[\exp(j\omega_1 X + j\omega_2 \dot{X})]$, rather than $p_{X\dot{X}}(x,\dot{x})$ as [16]

$$\begin{aligned} N_X(x_{\text{th}}) &= -\frac{1}{4\pi^2}\int_{-\infty}^{\infty}\int_{-\infty}^{\infty}\frac{1}{\omega_2}\frac{d\Phi_{X\dot{X}}(\omega_1,\omega_2)}{d\omega_2}e^{-j\omega_1 x_{\text{th}}}d\omega_1 d\omega_2, \\ &= -\frac{1}{4\pi^2}\int_{-\infty}^{\infty}\int_{-\infty}^{\infty}\frac{\Phi_{X\dot{X}}(\omega_1,\omega_2)-\Phi_X(\omega_1)}{\omega_2^2}e^{-j\omega_1 x_{\text{th}}}d\omega_1 d\omega_2. \end{aligned} \tag{29}$$

For the calculation of the outage probability, $\text{Prob}[0 \le X \le x_{\text{th}}]$, we use the Euler numerical technique presented in [28] and given by

$$\text{Prob}[0 \le X \le x_{\text{th}}] = \frac{2^{-Q}e^{A/2}}{x_{\text{th}}}\sum_{q=0}^{Q}\binom{Q}{q}\sum_{n=0}^{N+q}\frac{(-1)^n}{\beta_n}\mathcal{R}\left\{\frac{\mathcal{M}_X\left(-\frac{A+2\pi jn}{2x_{\text{th}}}\right)}{\frac{A+2\pi jn}{2x_{\text{th}}}}\right\}+\epsilon(A,N,Q), \tag{30}$$

with $\binom{Q}{q} = \frac{Q!}{(Q-q)!q!}$, $\mathcal{R}\{\cdot\}$ as the real part of its argument and

$$\beta_n = \begin{cases} 2 & n=0 \\ 1 & n=1,2,\cdots,N, \end{cases}$$

In (30), $\mathcal{M}_X(s) = E[\exp(sx)]$ is the moment generating function (MGF) of the random variable X, and the overall error term $\epsilon(A,Q,N)$ is approximately bounded by

$$|\epsilon(A,N,Q)| \le \frac{e^{-A}}{1-e^{-A}} + \left|\frac{2^{-Q}\,e^{A/2}}{x_{\text{th}}}\sum_{q=0}^{Q}(-1)^{N+1+q}\binom{Q}{q}\mathcal{R}\left\{\frac{\mathcal{M}_X\left(-\frac{A+2\pi j(N+q+1)}{2x_{\text{th}}}\right)}{\frac{A+2\pi j(N+q+1)}{2x_{\text{th}}}}\right\}\right|. \tag{31}$$

Choosing the proper value of A for a specific discretization error, N, and Q for a specific truncation error, gives the desired error bound.

B. Application to Non IID Diversity Paths

Let us represent $r_l(t)$ as $r_l(t) = x_l(t) + jy_l(t)$, where $x_l(t)$ and $y_l(t)$ are the inphase and quadrature components of the lth path, respectively. The process $x_l(t)$ is a real stationary

Gaussian process with mean a_l and the auto-covariance function $C_{x_l x_l}(\tau)$, while $y_l(t)$ is a zero-mean real stationary Gaussian process with the same auto-covariance function, i.e. $C_{y_l y_l}(\tau) = C_{x_l x_l}(\tau)$ (both have the same variance $b_{l,0}$). In general, for an arbitrary AOA distribution, $x_l(t)$ and $y_l(t)$ are correlated process with the cross-covariance function $C_{x_l y_l}(\tau) = -C_{y_l x_l}(\tau)$. It is easy to verify that $C_{r_l r_l}(\tau) = C_{x_l y_l}(\tau) + jC_{y_l y_l}(\tau)$ [2]. According to the statistical properties of $x_l(t)$ and $y_l(t)$, $\alpha_l(t) = |r_l(t)| = \sqrt{x_l^2(t) + y_l^2(t)}$ is a Rician process and for $a_l = 0$ it becomes a Rayleigh process. Based on (12), the total instantaneous SNR per symbol at the output of both MRC and postdetection EGC can be written as

$$\gamma(t) = \sum_{l=1}^{L} \gamma_l(t) = \frac{E_s}{N_0} \sum_{l=1}^{L} [x_l^2(t) + y_l^2(t)], \tag{32}$$

while for the derivative we have

$$\dot{\gamma}(t) = \sum_{l=1}^{L} \dot{\gamma}_l(t) = \frac{2E_s}{N_0} \sum_{l=1}^{L} [x_l(t)\dot{x}_l(t) + y_l(t)\dot{y}_l(t)]. \tag{33}$$

Given this set-up and under the fading independence assumption across the paths, we have $\Phi_{\gamma\dot{\gamma}}(\omega_1, \omega_2) = \prod_{l=1}^{L} \Phi_{\gamma_l \dot{\gamma}_l}(\omega_1, \omega_2)$ where (based on the Turin classical result on the CF of quadratic forms in Gaussian variables [29]) $\Phi_{\gamma_l \dot{\gamma}_l}(\omega_1, \omega_2)$ is given by [16]

$$\Phi_{\gamma_l \dot{\gamma}_l}(\omega_1, \omega_2) = \frac{\exp\left(-\frac{\gamma_s a_l^2 (2\gamma_s b_{l,2} \omega_2^2 - j\omega_1)}{1 + 4\gamma_s^2 (b_{l,0} b_{l,2} - b_{l,1}^2)\omega_2^2 - j2\gamma_s b_{l,0}\omega_1}\right)}{1 + 4\gamma_s^2 (b_{l,0} b_{l,2} - b_{l,1}^2)\omega_2^2 - j2\gamma_s b_{l,0}\omega_1}, \tag{34}$$

where we have defined $\gamma_s = E_s/N_0$ to simplify the notation of (34). For isotropic scattering which yields (8), we express (34) in terms of the Rician factor $K_l = a_l^2/(2b_{l,0})$ and the average power $\Omega_l = E[\alpha_l^2] = a_l^2 + 2b_{l,0}$, by substituting $a_l^2 = K_l\Omega_l/(K_l + 1)$ and $2b_{l,0} = \Omega_l/(K_l + 1)$ into (34) as

$$\Phi_{\gamma_l \dot{\gamma}_l}(\omega_1, \omega_2) = \frac{(K_l + 1)^2 \exp\left(-\frac{\bar{\gamma}_l K_l [2\pi^2 f_d^2 \bar{\gamma}_l \omega_2^2 - j(K_l + 1)\omega_1]}{(K_l + 1)^2 + 2\pi^2 f_d^2 \bar{\gamma}_l^2 \omega_2^2 - j\bar{\gamma}_l (K_l + 1)\omega_1}\right)}{(K_l + 1)^2 + 2\pi^2 f_d^2 \Omega^2 \omega_2^2 - j\bar{\gamma}_l (K_l + 1)\omega_1}. \tag{35}$$

When the lth path has a Rayleigh distribution, $a_l = 0$, (34) significantly simplifies to

$$\Phi_{\gamma_l \dot{\gamma}_l}(\omega_1, \omega_2) = \frac{1}{1 + 4\gamma_s^2 (b_{l,0} b_{l,2} - b_{l,1}^2)\omega_2^2 - j2\gamma_s b_{l,0}\omega_1}. \tag{36}$$

Furthermore, isotropic scattering reduces (37) to

$$\Phi_{\gamma_l \dot{\gamma}_l}(\omega_1, \omega_2) = \frac{1}{1 + 2\pi^2 f_d^2 \bar{\gamma}_l^2 \omega_2^2 - j\bar{\gamma}_l \omega_1}. \tag{37}$$

C. Numerical Examples

Through the application of the general expression in (34), together with (29), one can calculate $N_\gamma(\gamma_{\rm th})$ for many different generalized fading channels of practical interest, which seems to be intractable using the PDF-based approach. For example, Fig. 3 shows the LCR and AOD over independent Rayleigh fading paths with isotropic scattering and an exponentially decaying PDP ($\bar{\gamma}_l = \bar{\gamma}_1 \exp[-\delta(l-1)],\ l = 1, 2, ..., L$). Note that the unbalanced distribution of power among the branches, $\delta \neq 0$, increases the AOD. As another example, Fig. 4 shows the curves for a RAKE receiver with two and three fingers, experiencing non-isotropic scattering over a non-constant PDP. The parameter of Fig. 4 are taken from measured values reported in [30] and [31]. Specifically, for the two-finger RAKE receiver in [30], the first path is Rayleigh with $\mu_1 = 90°$ and $\kappa_1 = 0.77$, the second path is Rician with $\mu_2 = 105°$ and $\kappa_2 = 525$, and the power unbalance ratio ($\bar{\gamma}_2/\bar{\gamma}_1$) between the two fingers is 2.13. On the other hand, in the three-finger RAKE receiver [31], all the paths are Rician with $\mu_1 = -42°$, $\mu_2 = -11°$, $\mu_3 = 162°$, $\kappa_1 = \kappa_2 = \kappa_3 = 365$, $K_1 = K_2 = K_3 = 10$, and the PDP is given by $\bar{\gamma}_l = \bar{\gamma}_1 10^{-0.1(l-1)l}$, l=1,2, and 3. Clearly, none of these real-world scenarios can be handled by the traditional PDF-based approach.

Now we consider a non-i.i.d. branch case, which highlights the importance of the utilization of spatial information (as well as the temporal data). Consider a three-finger RAKE receiver, where the three equal-power narrowbeam ($\kappa_1 = \kappa_2 = \kappa_3 = \kappa = 365$) Rayleigh waves impinge the receiver from different but closely-spaced AOAs. $\theta_1 = 85°$, $\theta_2 = 90°$, and $\theta_3 = 95°$. If we combine the three waves without taking into account the differences between the AOAs, i.e., if we incorrectly assume that θ_1=θ_2=$\theta_3 = 90°$, then we get the AOD curve given in Fig. 5 However, if we identify the AOA of the waves by beamforming using an antenna array, then after combining we obtain the other AOD curve in Fig. 5, which is smaller than the former curve within several order of magnitudes. This simple example demonstrates how spatial processing using antenna arrays can reduce the effect of fading, by decreasing the AOD.

V. Conclusion

Relying on a PDF-based approach, this paper derived closed-form expressions for the AOD of MRC and EGC over i.i.d. Rayleigh and Rician fading channels. Numerical examples showed that non-isotropic scattering and the number of diversity paths have an important impact on the AOD. The paper presented also a CF-based numerical technique for the exact AOD evaluation of MRC over not necessarily i.i.d. Rayleigh and Rician fading channels. The analysis was illustrated by numerical results/plots which showed that the power delay profile, the angle of arrivals, and the angle spreads have a non-negligible effect on the AOD of diversity systems operating over typical fading channels of practical interest.

References

[1] W. C. Jakes, *Microwave Mobile Communications.* Piscataway, NJ: IEEE, second ed., 1994.

[2] G. L. Stüber, *Principles of Mobile Communications.* Boston, MA: Kluwer Academic Publishers, 1996.

[3] T. S. Rappaport, *Wireless Communications: Principles and Practice.* Prentice Hall PTR, 1996.

[4] M. -S. Alouini and A. Goldsmith, "A unified approach for calculating the error rates of linearly modulated signals over generalized fading channels," *IEEE Trans. Commun.*, vol. 47, pp. 1324–1334, September 1999.

[5] M. K. Simon and M. -S. Alouini, "A unified approach for the probability of error for noncoherent and differentially coherent modulations over generalized fading channels," *IEEE Trans. Commun.*, vol. 46., pp. 1625–1638, December 1998.

[6] A. J. Goldsmith and S. G. Chua, "Variable-rate variable-power M-QAM for fading channels," *IEEE Trans. Commun.*, vol. 45, pp. 1218–1230, October 1997.

[7] A. Goldsmith and S. G. Chua, "Adaptive coded modulation for fading channels," *IEEE Trans. Commun.*, vol. COM-46, pp. 595–602, May 1998.

[8] M. -S. Alouini and A. Goldsmith, "Adaptive M-QAM modulation over Nakagami fading channels," in *Proc. Communication Theory Mini-Conference (CTMC-VI) in conjunction with IEEE Global Commun. Conf. (GLOBECOM'97), Phoenix, AZ*, pp. 218–223, November 1997.

[9] M. -S. Alouini, X. Tang, and A. Goldsmith, "An adaptive modulation scheme for simultaneous voice and data transmission over fading channels," *IEEE J. Select. Areas Commun.*, vol. SAC-17, pp. 837–850, May 1999.

[10] W. C. Y. Lee, "Level crossing rates of an equal-gain predection diversity comboiner," *IEEE Trans. Commun.*, vol. 18, pp. 417–426, August 1970.

[11] W. C. Y. Lee, "Mobile radio performance for a two-branch equal-gain combining receiver with correlated signals at the land site," *IEEE Trans. Veh. Technol.*, vol. 27, pp. 239–243, November 1978.

[12] M. F. Adachi and J. D. Parsons, "Effects of correlated fading on level crossing rates and average fade durations with predetection diversity reception," *IEE Proc.F, Commun., Radar, Signal Processing*, vol. 135, pp. 11–17, Feburary 1988.

[13] S. Mukherjee and H. Viswanathan, "Minimum duration outages for diversity systems," in *Proc. IEEE Global Telecommu. Conf. (GLOBECOM'98), Sydney, Australia*, pp. 3663–3668, Nov 1998.

[14] M. D. Yacoub, J. E. Vargas Bautista, and L. G. de Rezende Guedes, "On higher order statistics of the Nakagami-m distribution," *IEEE Trans. Veh. Technol.*, vol. 48, pp. 790–793, May 1999.

[15] N. Youssef, T. Munakata, and M. Takeda, "Fade statistics in Nakagami fading environments," in *Proc. IEEE Int. Symp. Spread Spectrum Techniques and Applications, Mainz, Germany*, pp. 1244–1247, 1996.

[16] A. Abdi and M. Kaveh, "Level crossing rate in terms of the characteristic function: A new approach for calculating the fading rate in diversity systems," *IEEE Trans. Commun.*, vol. 50, September 2002.

[17] A. Abdi, A. Barger, and M. Kaveh, "A parametric model for the distribution of the angle of arrival and the associated correlation function and power spectrum at the mobile station," *IEEE Trans. Veh. Technol.*, vol. 51, pp. 425–434, May 2002.

[18] K. V. Mardia, *Statistics of Directional Data.* London: Academic, 1972.

[19] I. S. Gradshteyn and I. M. Ryzhik, *Table of Integrals, Series, and Products.* San Diego, CA: Academic, fifth ed., 1994.

[20] J. Komaili, L. A. Ferrari, and P. V. Sankar, "Estimating the bandwidth of a normal process from the level crossings of its envelope," *IEEE Trans. Acoustics, Speech, and Signal processing*, vol. 10, pp. 1481–1483, October 1987.

[21] M. K. Simon, S. M. Hinedi, and W. C. Lindsey, *Digital Communication Techniques- Signal Design and Detection.* Englewood Cliffs, NJ: PTR Prentice Hall, 1995.

[22] Y. C. Ko, A. Abdi, M. S. Alouini, and M. Kaveh, "Average outage duration of diversity systems over generalized fading channels," in *Proc. IEEE Wireless Commun. and Net. Conf. (WCNC'2000), Chicago, IL*, pp. 216–221, September 2000.

[23] M. D. Yacoub, C. R. C. M. da Silva, and J. E. Vargas B., "Second-order statistics for equal gain and maximal ratio diveristy-combining reception," *Electron. Lett.*, vol. 36, pp. 382–384, February 2000.

[24] X. Qi, M. -S. Alouini, and Y. -C. Ko, "Closed-form analysis of dual-diversity equal-gain combiners over Rayleigh channels," in *Proc. IEEE Veh. Technol. Conf. (VTC'Spring 02), Birmingham, AL*, pp. 1559–1563, May 2002.

[25] N.-C. Beaulieu, "An infinite series for the computation of the complementary probability distribution function of a sum of independent random variables and its application to the sum of Rayleigh random variables," *IEEE Commun. Commun.*, vol. COM-26, pp. 1463–1474, September 1990.

[26] N. C. Beaulieu and A. A. Abu-Dayya, "Analysis of equal gain diversity on Nakagami fading channels," *IEEE Trans. Commun.*, vol. COM-39, pp. 225–234, February 1991.

[27] A.-A. Abu-Dayya and N.-C. Beaulieu, "Microdiversity on Rician fading channels," *IEEE Commun. Commun.*, vol. COM-42, pp. 2258–2267, June 1994.

[28] Y. -C. Ko, M. -S. Alouini, and M. K. Simon, "An MGF-based numerical technique for the outage probability evaluation of diversity systems," *IEEE Trans. Commun.*, vol. 49, pp. 12–14, September 2000.

[29] G. L. Turin, "The characteristic function of Hermitian quadratic forms in complex normal variables," *Biometrika*, vol. 47, pp. 199–201, 1960.

[30] P. C. Fannin and A. Molina, “Analysis of mobile radio channel sounding measurements in inner city Dublin at 1.808GHz,” *IEE Proc. Commun*, vol. 143, pp. 311–316, 1996.

[31] J. P. Rossi, J. P. Barbot, and A. J. Levy, “Theory and measurement of the angle of arrival and time delay of UHF radiowaves using a ring array,” *IEEE Trans. Antennas Propagat.*, vol. 45, pp. 876–884, May 1997.

FIGURES CAPTIONS

1. Fig. 1: Normalized LCR and AOD with MRC or postdetection EGC RAKE reception (L=1, 2, and 4), versus the normalized power threshold, $\gamma_{\text{th}}/\bar{\gamma}_1$, for two different scattering scenarios $(\mu_1, \kappa_1) = (0^\circ, 1.2)$ and $(0^\circ, 3.3)$, with i.i.d. Rayleigh diversity paths.
2. Fig. 2: Normalized LCR and AOD with MRC or postdetection EGC RAKE reception (L=1, 2, 3, and 4), versus normalized power threshold, $\gamma_{\text{th}}/\bar{\gamma}_1$, for isotropic scattering over i.i.d. Rician diversity paths with K=3dB.
3. Fig. 3: Normalized LCR and AOD of MRC or postdetection EGC RAKE reception (L=2 and 4), versus the normalized power threshold, $\gamma_{\text{th}}/\bar{\gamma}_1$, over independent Rayleigh fading paths with isotropic scattering and an exponentially decaying power delay profile, $\bar{\gamma}_l = \bar{\gamma}_1 \exp[-\delta(l-1)]$, $l = 1, 2, ..., L$.
4. Fig. 4: Normalized LCR and AOD with MRC or postdetection EGC RAKE reception (L=2 and 3), versus the normalized power threshold, $\gamma_{\text{th}}/\bar{\gamma}_1$, over two different generalized fading channels (Rayleigh/Rician and Rician/Rician/Rician), with parameters derived from published empirical results in [**30**] and [**31**], respectively.
5. Fig. 5: Normalized LCR and AOD with MRC or postdetection EGC RAKE reception (L=4), versus the normalized power threshold, $\gamma_{\text{th}}/\gamma_1$, for different angle of arrivals.

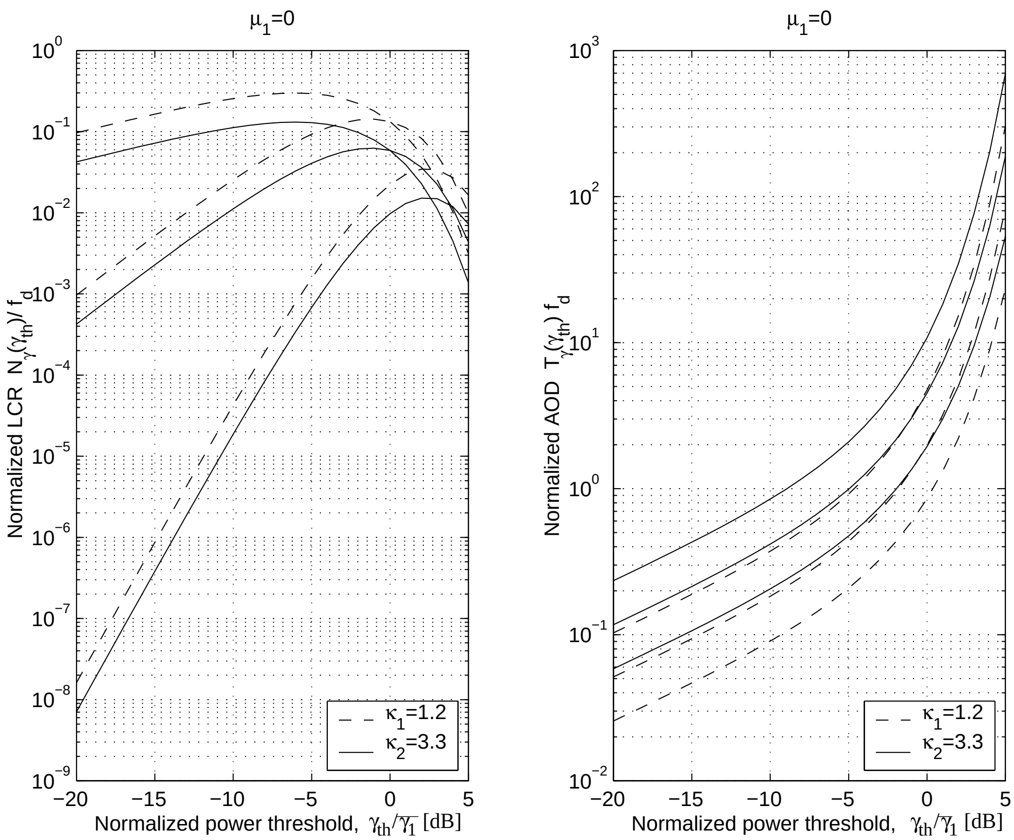

μ1=0
Normalized LCR N_γ(γ_th)/ f_d
Normalized power threshold, γ_th/γ̄_1 [dB]
κ1=1.2
κ2=3.3
μ1=0
Normalized AOD T_γ(γ_th) f_d
Normalized power threshold, γ_th/γ̄_1 [dB]
κ1=1.2
κ2=3.3

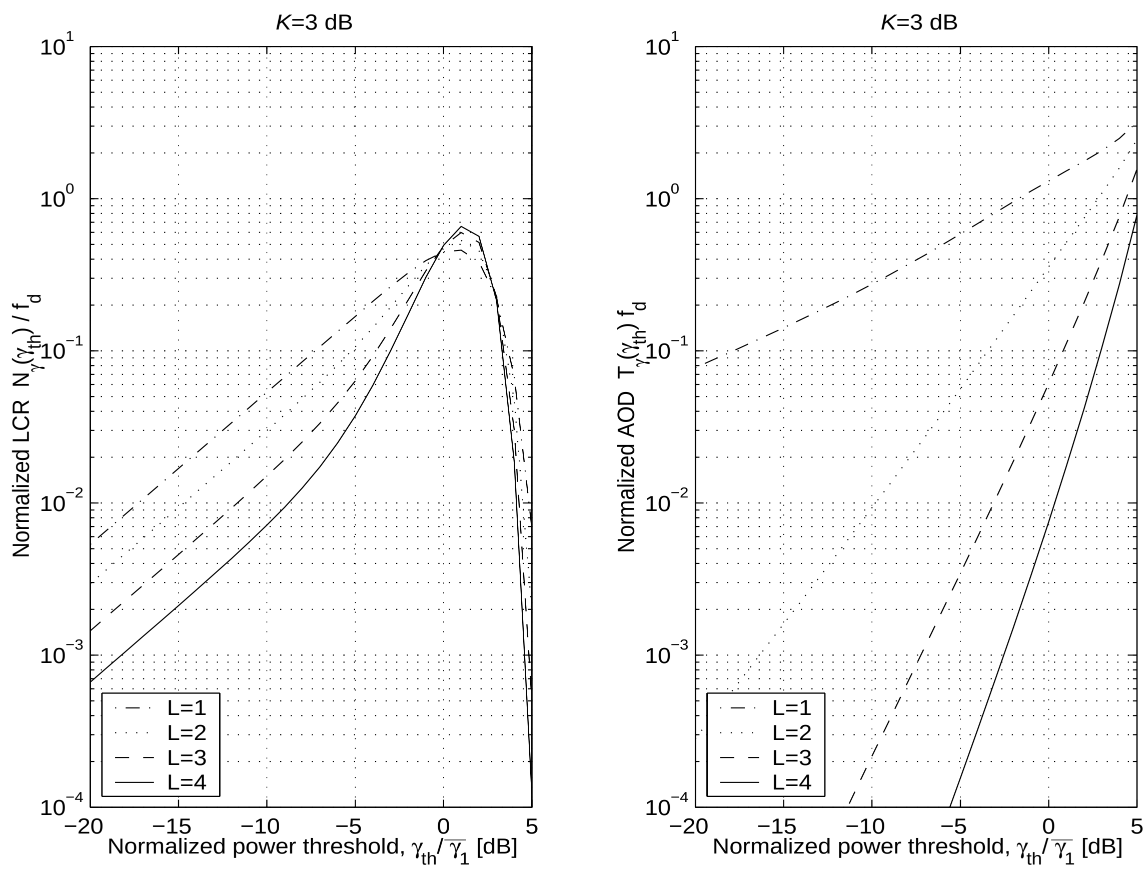
K=3 dB
Normalized LCR $N_\gamma(\gamma_{th})$ / f_d
Normalized power threshold, $\gamma_{th}/\overline{\gamma_1}$ [dB]
L=1
L=2
L=3
L=4
K=3 dB
Normalized AOD $T_\gamma(\gamma_{th})$ f_d
Normalized power threshold, $\gamma_{th}/\overline{\gamma_1}$ [dB]
L=1
L=2
L=3
L=4

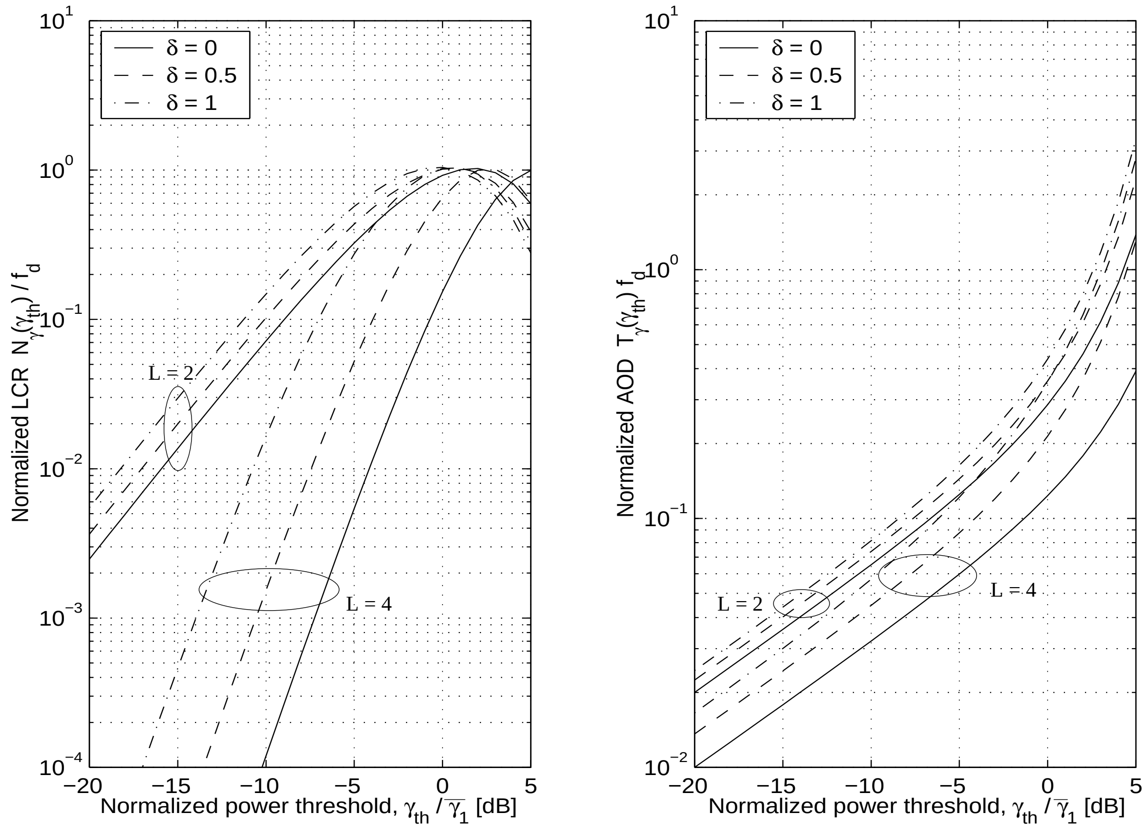
δ = 0
δ = 0.5
δ = 1
L = 2
L = 4
Normalized LCR $N_\gamma(\gamma_{th}) / f_d$
Normalized power threshold, $\gamma_{th} / \overline{\gamma}_1$ [dB]
Normalized AOD $T_\gamma(\gamma_{th}) f_d$
Normalized power threshold, $\gamma_{th} / \overline{\gamma}_1$ [dB]

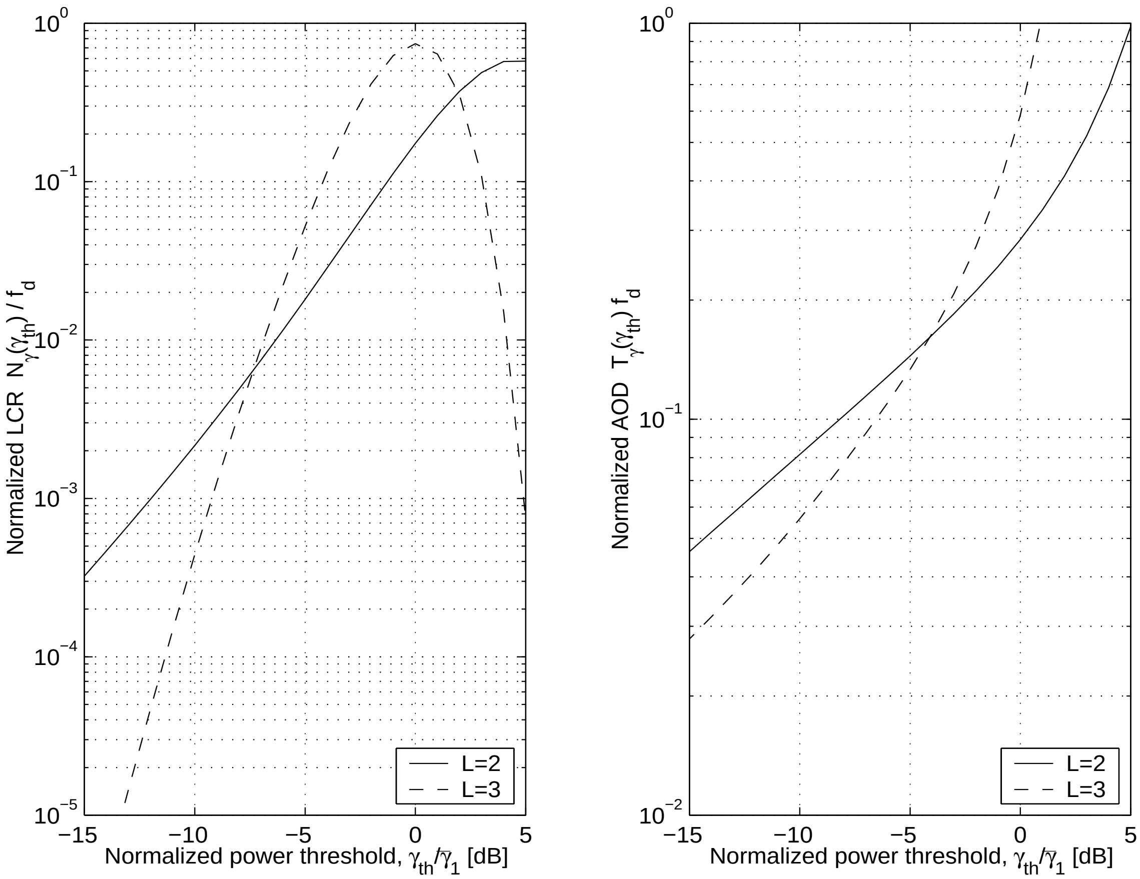
Normalized LCR $N_\gamma(\gamma_{th})$ / f_d
Normalized power threshold, $\gamma_{th}/\bar{\gamma}_1$ [dB]
L=2
L=3
Normalized AOD $T_\gamma(\gamma_{th})$ f_d
Normalized power threshold, $\gamma_{th}/\bar{\gamma}_1$ [dB]
L=2
L=3

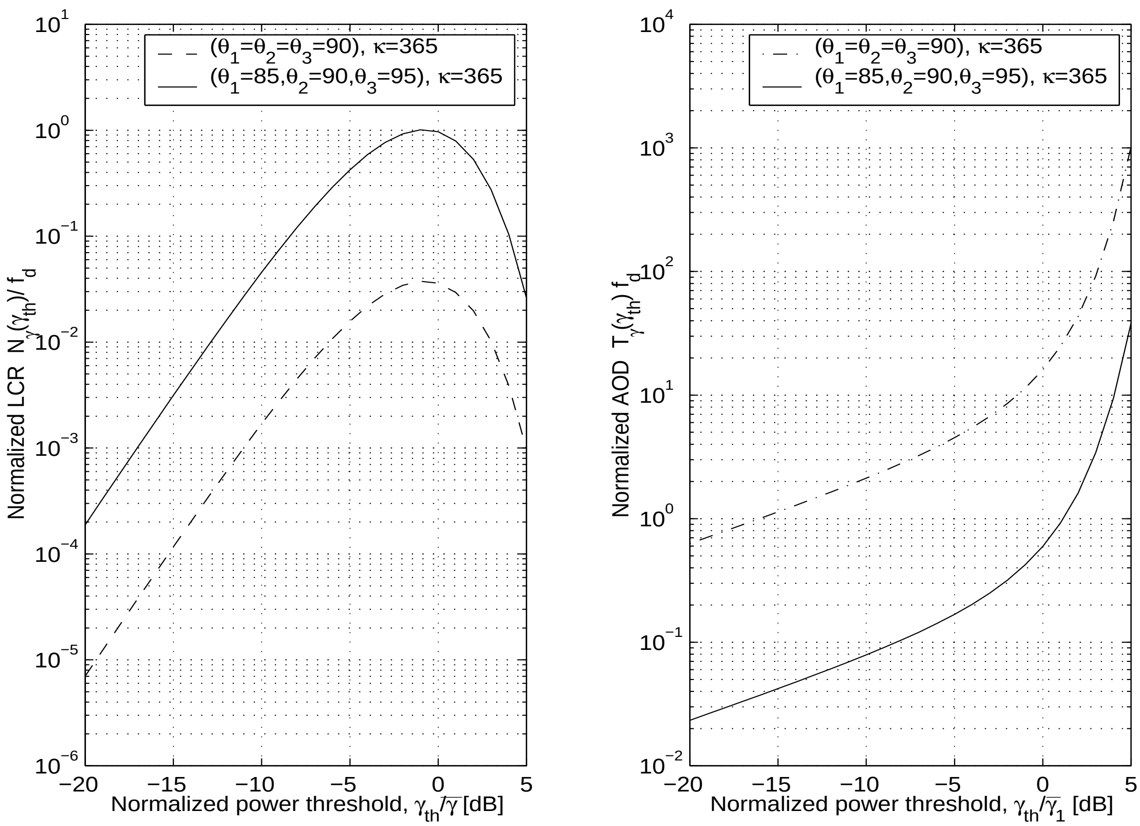
(θ1=θ2=θ3=90), κ=365
(θ1=85,θ2=90,θ3=95), κ=365
Normalized LCR Nγ(γth)/ fd
Normalized power threshold, γth/γ̄ [dB]
Normalized AOD Tγ(γth) fd
Normalized power threshold, γth/γ̄1 [dB]